08

High-frequency EPR spectroscopy of paramagnetic manganese centers in GaAs : Mn crystals

© *R.A. Babunts, A.S. Gurin, I.V. Ilyin, A.P. Bundakova, M.V. Muzafarova,*
  A.G. Badalyan, N.G. Romanov[¶], P.G. Baranov

Ioffe Institute,
St. Petersburg, Rusia

[¶] E-mail: nikolai.romanov@mail.ioffe.ru

High-frequency electron paramagnetic resonance (EPR) is used to study the unique properties of manganese centers in a GaAs : Mn crystal in strong magnetic fields at low temperatures. At frequencies of 94 and 130 GHz, EPR transitions were recorded in the Mn_{Ga}^{2+}-SH complex, which is a manganese ion with spin $S = 5/2$, which replaces gallium (Mn_{Ga}^{2+}) and an ionized acceptor (A^-) associated via an isotropic antiferromagnetic exchange interaction with a shallow hole (SH) with angular momentum $J = 3/2$. A complex system of energy levels of this complex in a magnetic field and the possibility of accurately determining exchange interactions from EPR spectra are analyzed. Another complex was investigated, in which an ionized acceptor Mn_{Ga}^{2+} interacts with a localized hole center in the form of a diamagnetic ion O^{2-} replacing As. This complex, $Mn_{Ga}^{2+}-O_{As}^{2-}$, is characterized by axial symmetry along the $\langle 111 \rangle$ axis of the cubic GaAs crystal and an anisotropic EPR spectrum. Due to the high Boltzmann factor, in our studies, the order of the fine structure spin levels of this complex was determined. The effect of the Boltzmann populations of the energy levels on the high-frequency EPR spectra was also demonstrated for the Mn_{Ga}^{2+}-SH complex.

Keywords: high-frequency EPR, GaAs crystal, Mn acceptor, shallow hole, exchange interaction.

1. Introduction

Almost all applications of semiconductor materials require the introduction of electrically active impurities that either establish electron (n) and hole (p) conductivity or render doped semiconductors semi-insulating. The progress in spintronics, which is a novel area of research, dictates the need to introduce magnetic materials into device structures, but such applications are limited by the compatibility of magnetic materials with basic semiconductor materials (e.g., GaAs). A natural line of development in this field is the doping of semiconductors with magnetic impurities and synthesis of the so-called „semimagnetic" semiconductors with their magnetic properties manifested directly inside the semiconductor material. When used in electronic and optical devices, these semiconductors provide an additional degree of freedom associated with the spin of carriers. Since magnetic impurities in the form of ions of transition elements may be introduced into II−VI semiconductors in high concentrations, the research inside semimagnetic semiconductors was focused on these compounds [1–3]. However, the GaAs : Mn system is presently considered to be the most promising. While remaining a p-type semiconductor material, it exhibits ferromagnetic properties at fairly high temperatures [4,5]. Direct-band-gap semiconductor GaAs with a band gap of 1.43 eV is the base material used in optoelectronics to establish optical coupling with both electronic devices and optical emitters operating at room temperature. Several types of paramagnetic manganese centers can be found in GaAs : Mn. The key among them is an unusual system in the form of a Mn^{2+} ion that replaces Ga and is an acceptor Mn_{Ga}^{2+} (A^-) coupled via the isotropic exchange interaction to a delocalized hole with shallow levels [6–9]. A shallow acceptor with a magnetic ion coupled directly to an electrically active acceptor is thus produced (see review [9]).

Since diluted magnetic semiconductor (Ga, Mn)As [5] is compatible with common GaAs, it is regarded as an ideal material for research and possible applications in spintronics. Thus, Mn doping impurities in GaAs serve as shallow acceptors that simultaneously produce a magnetic ion and a hole. Ferromagnetism emerges in GaAs : Mn if the concentration of doping Mn^{2+} magnetic ions exceeds 1%. It is believed that the ferromagnetic coupling between spins $S = 5/2$ of Mn^{2+} ions is induced by the presence of delocalized holes, which serve as a „glue" [10].

The aim of the present study is to examine the properties of manganese centers in strong magnetic fields at low temperatures (i.e., in such conditions when, in accordance with the Boltzmann distribution, only the lower spin levels are populated).

2. Experimental procedure

A bulk GaAs : Mn crystal was grown by the Czochralski method and doped with Mn to a concentration of $\sim 10^{18}$ cm^{-3}. A puck-shaped blank was grown in the [111]
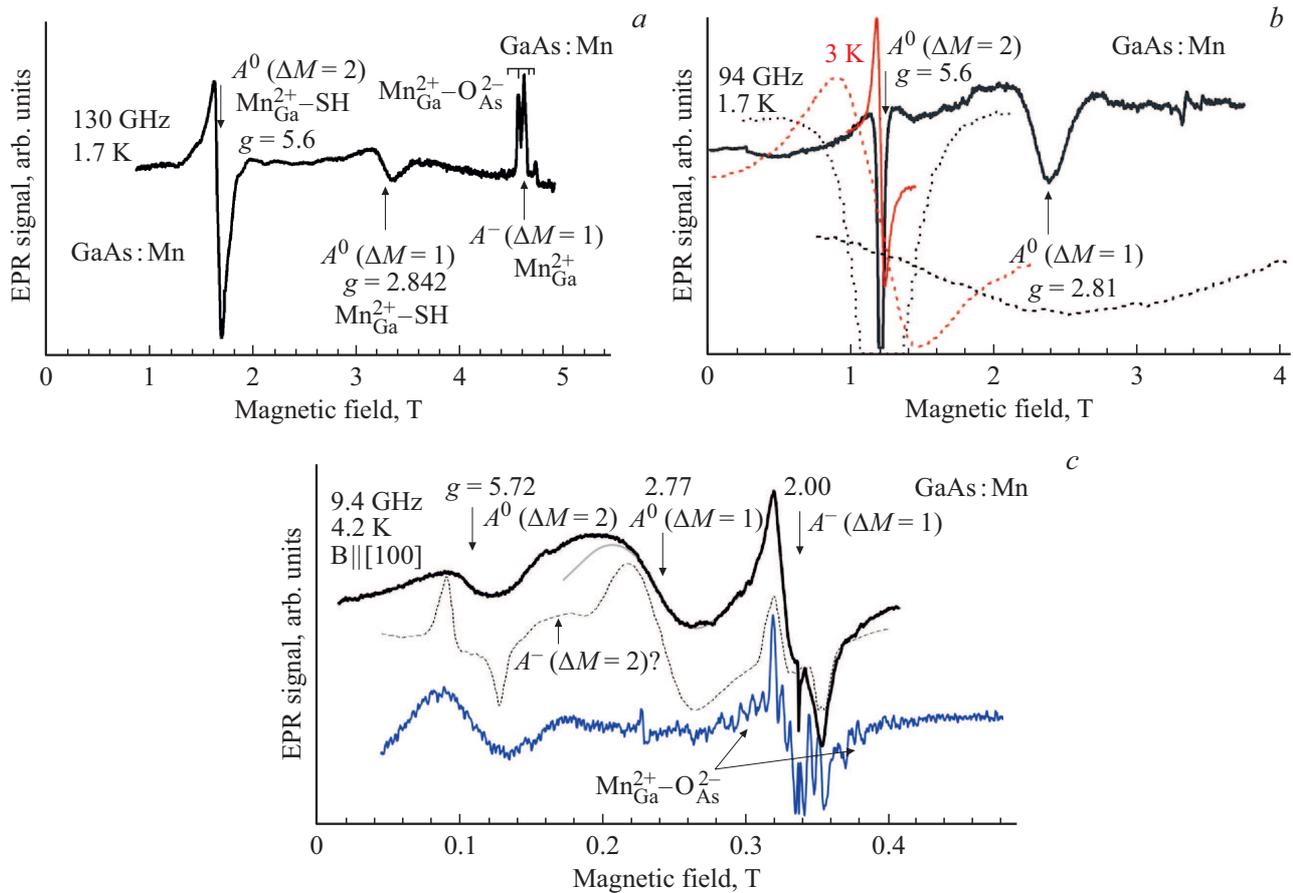
Figure 1. EPR spectra of manganese centers in the GaAs : Mn crystal measured in three bands at a temperature of $1.7-4.2$ K: (*a*) 2 mm, 130 GHz; (*b*) 3 mm, 94 GHz (the red curve corresponds to the forbidden transition detected at 3 K); (*c*) 3 cm, 9.4 GHz. Three types of manganese centers were detected: (i) Mn^{2+} ion occupying the position of Ga, Mn_{Ga}^{2+}, and acting as a negatively charged acceptor A^- that captures a shallow hole delocalized around Mn_{Ga}^{2+} as a Coulomb attraction center, Mn_{Ga}^{2+}-SH; (ii) Mn_{Ga}^{2+} ion acting as a negatively charged acceptor A^-; (iii) Mn_{Ga}^{2+} ion with oxygen in nonparamagnetic state O^{2-}, which replaces As (O_{As}^{2-}), located in its nearest-neighbor environment along the molecular bond of the tetrahedron in the $\langle 111 \rangle$ direction, Mn_{Ga}^{2+}-O_{As}^{2-} complex. Panel (*c*) shows the EPR spectra measured in the 3 cm band in the same sample and in an additional sample with a resolved hyperfine structure observed both for Mn_{Ga}^{2+} ions in defect-free environment and for Mn_{Ga}^{2+}-O_{As}^{2-} complexes. The dashed curve represents the spectrum similar to the one obtained in [6], where EPR spectra for Mn_{Ga}^{2+}-SH complexes were measured in the standard 3 cm band. The EPR spectra for Mn_{Ga}^{2+}-SH complexes at a frequency of 94 GHz (allowed transitions separated from forbidden ones) are shown for comparison in panel (*b*) on the same scale that is used in panel (*c*) for spectra in the 3 cm band (i.e., scale that is ten times smaller).

direction. Parallelepipedal samples $\sim 3 \times 3 \times 1$ mm in size were cut out of it and positioned so that they could be rotated about an edge coinciding with one of the $\langle 110 \rangle$ directions of the crystal.

EPR measurements were carried out in three bands: the standard one (3 cm, 9.4 GHz) and two high-frequency bands (3 mm, 94 GHz and 2 mm, 130 GHz). A spectrometer constructed at the Ioffe Institute in collaboration with the DOK company was used to measure the EPR spectra in the high-frequency 3-mm and 2-mm bands. This spectrometer operates in continuous and pulsed modes; the range of variation of magnetic fields is $0-7$ T, and the temperature variation range is $1.5-300$ K. A mode of EPR spectra measurement with low-frequency modulation of frequency was added as a complement to the standard measurement

procedure with low-frequency modulation of the magnetic field. This complementary mode is preferable for operation in strong magnetic fields, since the noise associated with the influence of strong magnetic fields on modulation coils is eliminated.

3. Experimental results and discussion

Fig. 1 presents the EPR spectra of manganese centers in the GaAs : Mn crystal measured at $1.7-4.2$ K in three bands: high-frequency 2 mm, 130 GHz (*a*) and 3 mm, 94 GHz (*b*) bands and the standard 3 cm, 9.4 GHz band (*c*). Three types of manganese centers were detected: (i) Mn^{2+} ions occupying the positions of Ga, Mn_{Ga}^{2+}, and acting as negatively charged acceptors A^- that capture a shallow
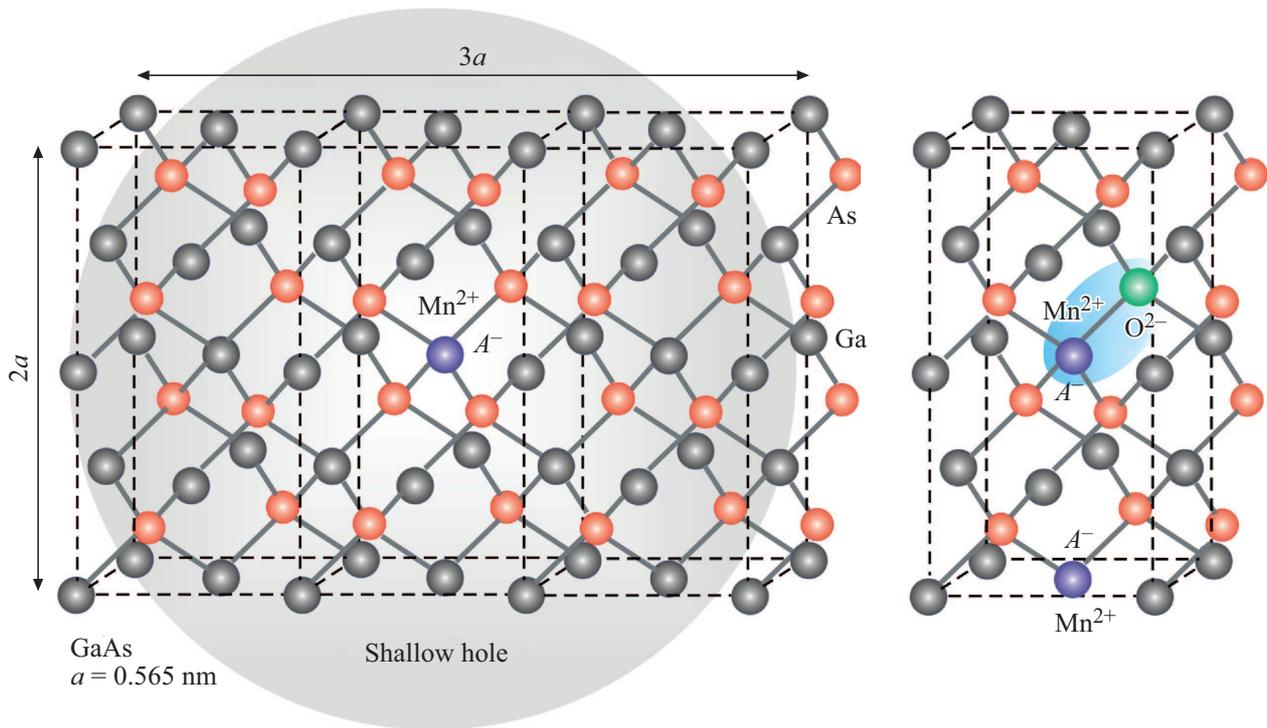
Figure 2. Models of three manganese centers in the GaAs:Mn crystals: (left panel) the Mn_{Ga}^{2+}-SH complex; (right panel) Mn_{Ga}^{2+} in defect-free environment and the Mn_{Ga}^{2+}-O_{As}^{2-} complex. The grey circle in the left panel denotes the spatial extent of a delocalized shallow hole within the crystal.

hole delocalized around Mn_{Ga}^{2+} as a Coulomb attraction center (Mn_{Ga}^{2+}-SH complex described above); (ii) Mn_{Ga}^{2+} ions acting as negatively charged acceptors A^- (Mn_{Ga}^{2+}); (iii) Mn^{2+} ion occupying the position of Ga, Mn_{Ga}^{2+}, and acting as a negatively charged acceptor A^- with oxygen in nonparamagnetic state O^{2-}, which replaces As-O_{As}^{2-}, located in its nearest-neighbor environment along the molecular bond of the tetrahedron in the $\langle 111 \rangle$ direction (Mn_{Ga}^{2+}-O_{As}^{2-} complex). Models of these three manganese centers are presented in Fig. 2. An approximate radius of a delocalized hole centered at a Mn_{Ga}^{2+} ion is also indicated in Fig. 2; according to [9], this radius is on the order of 1 nm. Thus, a shallow hole extends over several unit cells of the GaAs cubic crystal. It is particularly interesting to examine Mn_{Ga}^{2+}-SH complexes in nanostructures, since confinement effects are expected to manifest themselves there and alter the exchange interaction between the spin system of manganese and the angular momentum of a shallow hole. Fig. 1,c also shows the EPR spectra measured in the 3 cm band in an additional sample with a resolved hyperfine (HF) structure observed both for Mn_{Ga}^{2+} ions in defect-free environment and for Mn_{Ga}^{2+}-O_{As}^{2-} complexes. It can be seen that the magnitudes of HF splitting are roughly the same in both centers. Only the forbidden transition for Mn_{Ga}^{2+}-SH complex is observed in this sample; the allowed transition is not seen (likely due to strains in the crystal). A spectrum similar to the one obtained in [6], where EPR spectra for Mn_{Ga}^{2+}-SH complexes were measured in the standard 3 cm

band, is also shown for comparison in Fig. 1,c with a dashed curve. These measurements did not reveal directly the influence of the next (excited) state of the Mn_{Ga}^{2+}-SH complex with $F = 2$ on the EPR spectrum. Its presence was only hinted at by indirect data.

In the present study, measurements are performed in strong magnetic fields at low temperatures (i.e., in such conditions when only the lower spin levels are populated). This opens up the possibility of probing the complex system of energy levels of the Mn_{Ga}^{2+}-SH complex and the level system of the Mn_{Ga}^{2+}-O_{As}^{2-} complex. In both cases, the complexes have the form of a manganese center Mn_{Ga}^{2+} that is a negatively charged (ionized) acceptor A^- attracting either a delocalized shallow hole or a hole localized at the neighboring atom in the form of an impurity oxygen ion in the diamagnetic state (O_{As}^{2-}). The first complex yields an isotropic EPR spectrum, while the EPR spectrum in the second case is anisotropic.

Let us examine the Mn_{Ga}^{2+}-SH complex. The conventional model of this complex is a system where it is energetically favorable for a hole to remain on a delocalized orbit around acceptor A^- in the form of Mn_{Ga}^{2+} ($3d^5$), $S = 5/2$ (Fig. 2, left panel). The complex of Mn_{Ga}^{2+} and a shallow hole then forms due to the isotropic exchange interaction between electrons of the $3d^5$ shell of the Mn_{Ga}^{2+} ion ($S = 5/2$) and spins of the delocalized hole ($J = 3/2$). The end result is a shallow acceptor with a level depth on the order of 0.1 eV [6–9].

The EPR spectrum of the Mn_{Ga}^{2+}-SH complex in GaAs can be characterized by the following approximate spin Hamiltonian:

$$H = g_S \mu_B \mathbf{B} \cdot \mathbf{S} + g_J \mu_B \mathbf{B} \cdot \mathbf{J} + c\mathbf{S} \cdot \mathbf{J}, \quad (1)$$

where B is the magnetic field, $g_S = 2.00$ is the isotropic g-factor of acceptor Mn_{Ga}^{2+} ($3d^5$, $S = 5/2$), μ_B is the Bohr magneton, $g_J = 0.78$ is the g-factor of a shallow hole [11], and c is the isotropic exchange interaction between Mn_{Ga}^{2+} and the shallow hole.

Mn_{Ga}^{2+} with spin $S = 5/2$ is coupled in the examined complex by antiferromagnetic exchange interaction c (in the form of $c\mathbf{S} \cdot \mathbf{J}$) to a shallow hole with angular momentum $J = 3/2$. In accordance with the momentum summation rule, $\mathbf{F} = \mathbf{S} + \mathbf{J}$ ($F = 1, 2, 3, 4$), where, according to the Landé interval rule, $\Delta E_{F-(F-1)} = cF$; i.e., the intervals between levels in zero magnetic field are $2c$, $5c(2c + 3c)$, $9c(2c + 3c + 4c)$ from the lower level upwards. Thus, ground state $F = 1$ is obtained under the assumption of antiferromagnetic coupling between a hole and acceptor nucleus $3d^5$. The corresponding eigenvectors of state $F = 1$ in the $|M_S, M_J\rangle$ basis are calculated as follows [6,9]:

$$|1, +1\rangle = 1/2\sqrt{2}|5/2, -3/2\rangle - 1/10\sqrt{30}|3/2, -1/2\rangle$$
$$+ 1/10\sqrt{15}|1/2, 1/2\rangle - 1/10\sqrt{5}|-1/2, 3/2\rangle,$$

$$|1, 0\rangle = 1/5\sqrt{5}|3/2, -3/2\rangle - 1/10\sqrt{30}|1/2, -1/2\rangle$$
$$+ 1/10\sqrt{30}|-1/2, 1/2\rangle - 1/5\sqrt{5}|-3/2, 3/2\rangle,$$

$$|1, -1\rangle = -1/2\sqrt{2}|-5/2, 3/2\rangle + 1/10\sqrt{30}|-3/2, 1/2\rangle$$
$$- 1/10\sqrt{15}|-1/2, -1/2\rangle + 1/10\sqrt{5}|1/2, -3/2\rangle. \quad (2)$$

Calculating the isotropic g-factor with the use of wave functions of the lower triplet level with $F = 1$ (2), we find the following:

$$g_{F=1} \approx (7/4)g_S - (3/4)g_J \quad (3)$$

Inserting the values of g_S and g_J given above into (3), we obtain $g_{F=1} = 2.9$. This value agrees with the values of $g_{F=1} = 2.77$ (determined based on the EPR spectra [6]) and $g = 2.74$ (obtained using the spin-flip Raman scattering (SFRS) technique [12]), thus verifying the correctness of the used Mn_{Ga}^{2+}-SH model. Two lines corresponding to transitions $\Delta M_F = 1$ and $\Delta M_F = 2$ between the sublevels of ground state $F = 1$ with g-factors $g = 2.77$ and $g = 5.72$, respectively, were observed in the EPR spectra in [6].

Owing to random local strain, ground state $F = 1$ is split into two multiplets with projections $M_F = 0$ and $M_F = \pm 1$ of the total angular momentum onto the quantization axis. This splitting is smaller than the exchange energy of acceptor Mn, which was estimated to lie in the $4-6$ meV range based on the data of several indirect studies [13,14]. Direct SFRS measurements of the energy difference between states
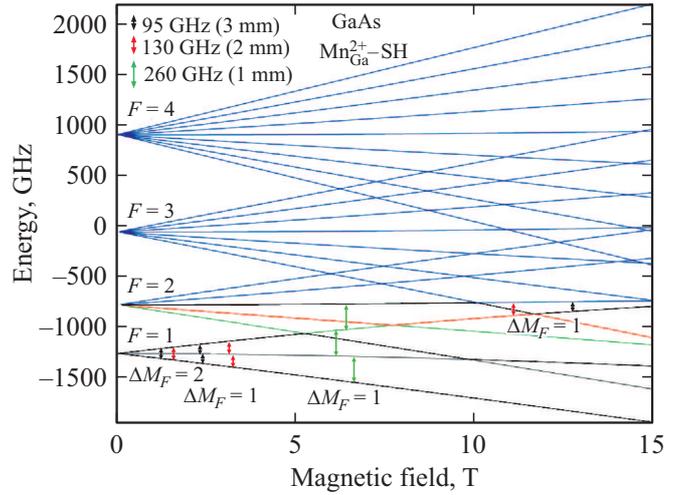

Figure 3. Diagram of energy levels for the Mn_{Ga}^{2+}-SH center that has the form of a Mn_{Ga}^{2+} ion with spin $S = 5/2$ coupled by antiferromagnetic exchange interaction c to a shallow hole with angular momentum $J = 3/2$. Each of the four levels $F = 1, 2, 3, 4$ in zero magnetic field (if splitting induced by strains in the crystal is ignored) is characterized by $2F + 1$-fold degeneracy, which is lifted by the magnetic field. Three transitions are seen in the 130 GHz band at low temperature in the studied range of magnetic fields: two allowed transitions in a field on the order of 3 T and one forbidden transition in a field that is two times weaker. Another allowed transition between levels $M_{F=1} = +1$ and $M_{F=2} = 0$ is seen in a field on the order of 12 T, but this transition lies outside the operating range of the EPR spectrometer. The transitions for the 94 GHz band are indicated as well. The results of calculation for the expected transitions in the 1 mm band at a frequency of 260 GHz are also shown.

$F = 1$ and $F = 2$ provided the following estimate of the exchange constant: $\Delta(F_1 - F_2) = 2.2$ meV (17 cm^{-1}) [12].

For comparison, allowed and forbidden transitions in the EPR spectra of Mn_{Ga}^{2+}-SH complexes at a frequency of 94 GHz are shown separately with dashed curves in Fig. 1, b on the same scale that is used in Fig. 1, c for spectra in the 3 cm band (i.e., scale that is ten times smaller). It can be seen that the widths of lines of the forbidden transition are almost the same, while the line of the allowed transition in the 3 mm band is significantly wider than the line in the 3 cm band. A small change in the width of the line of the forbidden transition corresponding to an order-of-magnitude increase in the field intensity is indicative of the fact that the Mn_{Ga}^{2+}-SH complex has a narrow spread of g-factors. The allowed transition is usually broadened greatly by strains in the crystal that induce splitting of the fine structure in the shallow hole state, which also causes splitting of the levels with $F = 1$ in zero magnetic field.

Fig. 3 presents the diagram of energy levels for the Mn_{Ga}^{2+}-SH center that has the form of Mn_{Ga}^{2+} with spin $S = 5/2$ coupled by antiferromagnetic exchange interaction c to a shallow hole with angular momentum $J = 3/2$. All four levels in zero magnetic field (if splitting induced
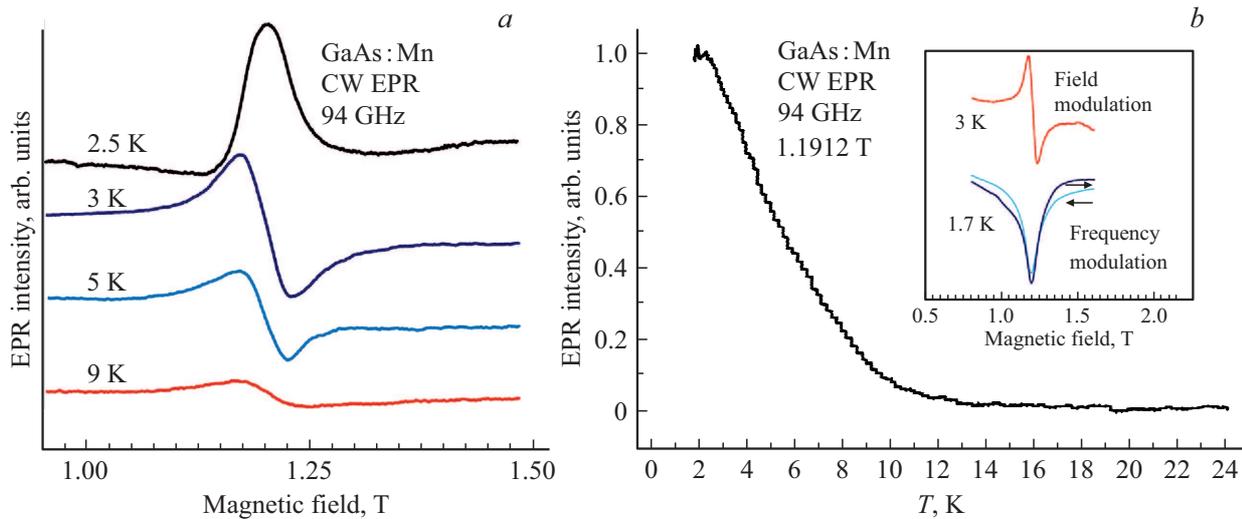
Figure 4. (*a*) Forbidden transition of Mn_{Ga}^{-}-SH EPR centers in the GaAs:Mn crystal recorded in the 3 mm band (94 GHz) at different temperatures. (*b*) Temperature dependence of the intensity of the signal of the Mn_{Ga}^{2+}-SH EPR center. EPR signals recorded with low-frequency modulation of the magnetic field and the frequency are shown in the inset. In both cases, the modulation frequency was 680 Hz. The spectra were measured with opposite sweep directions of the external magnetic field (indicated with arrows). Since ferromagnetic properties may be manifested in the GaAs:Mn system, the lack of hysteresis suggests that magnetic ordering does not occur in this case.

by strains in the crystal is ignored) are characterized by $2F + 1$-fold degeneracy, which is lifted by the magnetic field. The lower level with $F = 1$, which is a triplet, is split into sublevels with $M_F = +1, 0, -1$ in the magnetic field. We examine only the lowest triplet, since the higher levels are not populated under the conditions of the experiment. Three transitions are seen in the 130 GHz band in the studied range of magnetic fields: two allowed transitions in a field on the order of 3 T and one forbidden transition in a field that is two times weaker. These same transitions are observed experimentally for the Mn_{Ga}^{2+}-SH complex. It can be seen that the allowed transitions are split due to the nonlinearity of level $M_{F=1} = 0$ in the magnetic field: it deviates down from the horizontal line on the energy scale and thus shifts away in energy from level $M_{F=2} = 0$, which deviates toward higher energies. The magnitude of splitting of allowed transitions is associated directly with the influence of the upper level with $F = 2$; i.e., it is governed by the magnitude of exchange splitting. Owing to the large width of the line of allowed transitions (Fig. 1, *a, b*), which is attributable to strains in the crystal, this splitting could not be resolved in our experiments even in the 130 GHz band. Another allowed transition between levels $M_{F=1} = +1$ and $M_{F=2} = 0$ is seen at a frequency of 130 GHz in a field on the order of 12 T, but this transition lies outside the operating range of the EPR spectrometer. At a frequency of 94 GHz, this transition should be observed in even stronger fields. However, if the frequency is increased to 260 GHz (1 mm band), this allowed transition falls within the examined range of magnetic fields (see Fig. 3). EPR measurements in this band should allow one to determine accurately the magnitude of exchange interaction in the Mn_{Ga}^{2+}-SH complex.

Forbidden transitions $\Delta M_F = 2$ shown in Fig. 3 manifest themselves in calculations only if one sets such strains in the crystal that induce the splitting of levels $F = 1$ in zero magnetic field; however, the intensity of these transitions is extremely low. At the same time, we see that the forbidden transitions are very efficient even in strong magnetic fields (Fig. 1, *a, b*). This finding corroborates the assumption made in [15], namely that forbidden transitions are induced by the electric component of the microwave field. The wavelengths (2 and 3 mm) in our experiments are comparable to the sample size; therefore, both components of the microwave field can be involved in inducing the transitions between levels. Since the lines of magnetic-dipole transitions in EPR spectra should be several orders of magnitude less intense than the actual lines observed experimentally, a new EPR transition mechanism (electro-dipole) was proposed in [15] for the Mn_{Ga}^{2+}-SH system.

In fact, we consider this mechanism as possibly the most suitable, since the intensity of forbidden transition $\Delta M_F = 2$ obtained in simulations of EPR spectra was very low, and it was needed to add splitting of the fine structure, which is evidently present due to strains in the crystal, to the system with $J = 3/2$ in order for this transition to become discernible.

Fig. 4, *a* shows the forbidden transition of Mn_{Ga}^{2+}-SH EPR centers in the GaAs:Mn crystal recorded in the 3 mm band (95 GHz) at different temperatures. It can be seen that the intensity of the EPR signal decreases sharply as temperature increases. The temperature dependence of the intensity of the signal of the Mn_{Ga}^{2+}-SH EPR center is presented in Fig. 4, *b*. Note that the temperature of vanishing of the EPR spectrum of the examined complexes determined earlier in the standard 3 cm band [6] was on the order of $10-12$ K.

It thus follows from our research that this temperature does not depend on the measurement range of the spectra (i.e., on the magnetic field intensity). Presumably, this temperature is governed by the shallow level of the acceptor and its ionization at higher temperatures. EPR signals recorded with low-frequency modulation of the magnetic field and the frequency are shown in the inset of Fig. 4, *b*. In both cases, the modulation frequency was 680 Hz. The spectra were measured with opposite sweep directions of the external magnetic field (indicated with arrows). Since ferromagnetic properties may be manifested in the GaAs : Mn system, the lack of hysteresis suggests that magnetic ordering does not occur in this case. The concentration of manganese in the studied sample was apparently too low for such effects.

The EPR spectrum of the simplest defect (a Mn^{2+} ion occupying the position of Ga, Mn^{2+}_{Ga}, and acting as a negatively charged (ionized) acceptor A^-), which was examined earlier in the EPR experiments in [16,17], is characterized by the spin Hamiltonian with spin $S = 5/2$ of the following form:

$$H = g\mu_B \mathbf{B} \cdot \mathbf{S} + (1/6)a$$
$$\times [S_x^4 + S_y^4 + S_z^4 - 1/5 S(S+1)(3S^2 + 3S - 1)] + A\mathbf{I} \cdot \mathbf{S}. \quad (4)$$

The first term characterizes the Zeeman interaction; the second term, the interaction of the electron spin with the cubic crystal field; the last term, the hyperfine interaction of the magnetic moment of an electron and the nuclear magnetic moment of manganese (^{55}Mn, a natural abundance of 100%, $I = 5/2$). The parameters of the spin Hamiltonian are $|A| = 52.4 \cdot 10^{-4}\,cm^{-1}$ and $|a| = 14 \cdot 10^{-4}\,cm^{-1}$ [16,17]. These EPR signals are seen in Fig. 1, *a, b, c*; the hyperfine structure is also resolved in Fig. 1, *c*. The model of this center in the form of an isolated Mn^{2+}_{Ga} ion is presented in the right panel of Fig. 2.

Fig. 1, *a, b, c* shows the EPR spectrum of the complex based on acceptor Mn^{2+}_{Ga} interacting with a localized hole center in the form of a diamagnetic O^{2-}_{As} ion that replaces As. This complex, Mn^{2+}_{Ga}-O^{2-}_{As}, is characterized by axial symmetry along axis $\langle 111 \rangle$ of a cubic GaAs crystal with an anisotropic EPR spectrum and spin $S = 5/2$. Its EPR spectrum was measured earlier in [18,19]. Fig. 5, *a* shows the EPR spectrum of the Mn^{2+}_{Ga}-O^{2-}_{As} manganese complex in the GaAs : Mn crystal measured in the 2 mm band (130 GHz) at a low temperature of 1.7 K in a strong magnetic field (i.e., with a high Boltzmann factor). The Boltzmann distribution of populations is represented schematically in Fig. 5, *b* by different numbers of spheres.

The EPR spectrum of the Mn^{2+}_{Ga}-O^{2-}_{As} complex in GaAs may be characterized by the following spin Hamiltonian:

$$H = g\mu_B \mathbf{B} \cdot \mathbf{S} + D[S_z^2 - 1/3 S(S+1)] + A\mathbf{I} \cdot \mathbf{S}, \quad (5)$$

where B is the magnetic field, $g = 2.00$ is the isotropic g-factor, μ_B is the Bohr magneton, D is the fine-structure
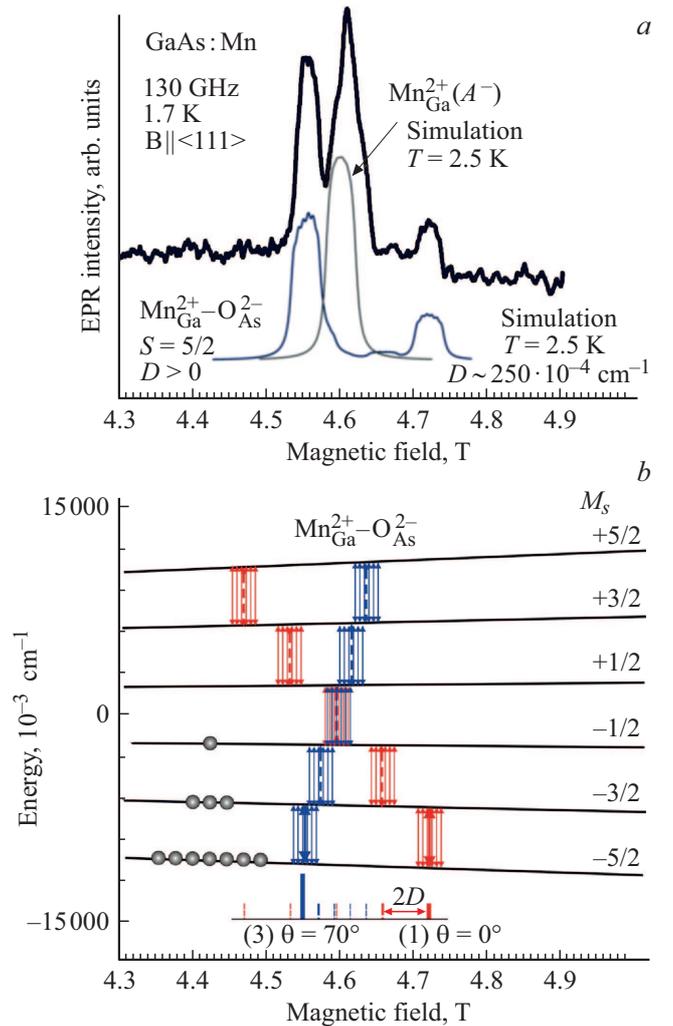
Figure 5. (*a*) EPR spectrum of Mn^{2+}_{Ga}-O^{2-}_{As} manganese complexes in the GaAs : Mn crystal measured in the 2 mm band (130 GHz) at a low temperature of 1.7 K (i.e., with a high Boltzmann factor). (*b*) Diagram of levels for four Mn^{2+}_{Ga}-O^{2-}_{As} centers with the magnetic field oriented along one of the equivalent $\langle 111 \rangle$ directions in a cubic GaAs crystal (the difference between levels for each of the four centers is within the line width on the diagram). In the context of a high Boltzmann factor (represented by a varying number of spheres), the microwave energy is absorbed efficiently only in the transitions between lower levels $-5/2 \to -3/2$; the absorption intensity for the other transitions should drop sharply. This effect was observed experimentally and is seen in the simulated spectrum shown at the bottom in panel (*a*). The intense signal in the region of $g = 2.00$ belongs to Mn^{2+}_{Ga} (A^-) centers in defect-free environment.

parameter, A is the isotropic hyperfine interaction constant, and $S = 5/2$ and $I = 5/2$ are the electron and nuclear spins.

The calculated energy levels and EPR transitions at a frequency of 130 GHz for the Mn^{2+}_{Ga}-O^{2-}_{As} complex shown in Fig. 5, *b* correspond to the orientation of the magnetic field parallel to the center axis coinciding with one of the four possible orientations of the complex along one of the molecular bonds in the GaAs crystal tetrahedron. Six allowed

transitions $\Delta M_S = \pm 1$ are shown, $\Delta m_I = 0$ correspond to nuclear transitions m_I: $5/2 \rightarrow 5/2$, $3/2 \rightarrow 3/2$, $1/2 \rightarrow 1/2$, $-1/2 \rightarrow -1/2$, $-3/2 \rightarrow -3/2$, and $-5/2 \rightarrow -5/2$. The ViewEPR program developed by V. Grachev was used in these calculations.

Fig. 5, b presents the energy levels of the axial Mn_{Ga}^{2+}-O_{As}^{2-} complex, $S = 5/2$, $I = 5/2$ for the magnetic field parallel to one of the $\langle 111 \rangle$ axes. The symmetry axis of one of the four possible complexes coincides with the direction of the magnetic field, and the magnitude of splitting of the fine structure reaches its maximum of 2D between the neighboring transitions. These transitions are marked with red in Fig. 5, b. The orientations of the center axis for the three remaining complexes make an angle of $110°$ ($70°$); their transitions coincide and are marked with blue in Fig. 5, b. The following parameters of the spin Hamiltonian were used in calculations: $g = 2.00$, $A = 53 \cdot 10^{-4}\,\mathrm{cm}^{-1}$, and $D = 250 \cdot 10^{-4}\,\mathrm{cm}^{-1}$.

Under thermal equilibrium, the populations of levels are governed by the Boltzmann distribution. Therefore, the lower levels are populated preferentially at lower temperatures, and EPR transitions $-5/2 \leftrightarrow -3/2$ are more intense. This results in the asymmetry of EPR spectra: when the field is oriented parallel to the center axis, high-field HF interaction series with the centroid shifted by 4D toward higher fields relative to $g = 2.00$ should have the maximum amplitude, while the series with the centroid shifted by 2D toward lower fields should have the maximum amplitude in the case of perpendicular orientation ($\theta = 90°$). With the orientation for three complexes with angle $\theta = 70°$ implemented in our experiments, the outermost line is shifted by a distance slightly shorter than 2D from the center. The more intense lines in Fig. 5, b are solid, while the lower-intensity transitions are shown with dashed lines (exclusive of the HF-0 structure). The EPR spectrum simulated for a temperature of 1.7 K is shown at the bottom in Fig. 5, a. Two intense signals corresponding to transitions $M_S = -5/2 \rightarrow M_S = 3/2$ for two angles $\theta = 0°$ and $\theta = 70°$ are seen. It should be noted that the ratio of intensities of the two outermost components for signals $\theta = 0°$ at distances 4D and 2D from the center provide data on the temperature of measurement of EPR spectra (in the region of temperatures below 10 K).

Fig. 6 illustrates the influence of temperature, which is due to the Boltzmann distribution of populations of spin levels in strong magnetic fields, on the EPR spectra of Mn_{Ga}^{2+}-O_{As}^{2-} in GaAs. The EPR spectra of Mn_{Ga}^{2+}-O_{As}^{2-} complexes and ionized Mn_{Ga}^{2+} acceptors were simulated at two temperatures; a line width of 2 mT, which is 2.5 times smaller than the one used to simulate the spectrum in Fig. 5, a, was used to reveal for illustration purposes the resolved hyperfine structure of manganese. It can be seen that as the temperature grows, the intensity of transition $-3/2 \rightarrow -1/2$ for orientation $\theta = 0°$ increases, the outermost transition $+3/2 \rightarrow +5/2$ starts to manifest
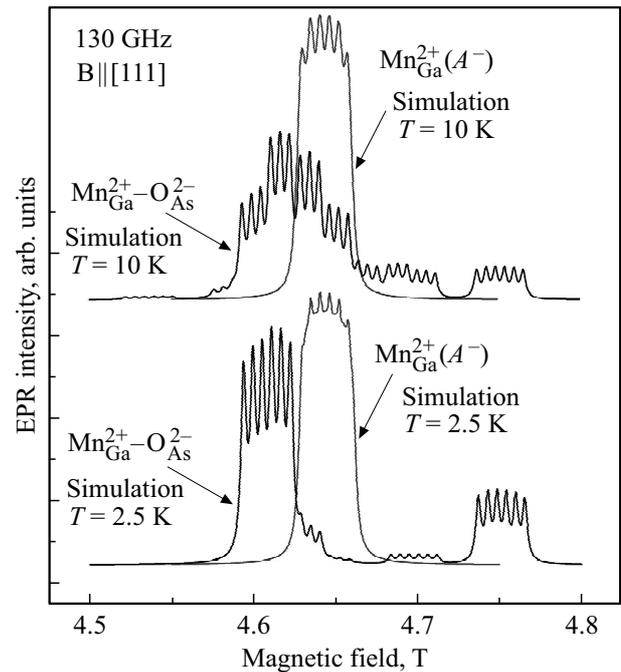
Figure 6. Illustration of the influence of temperature, which is due to the Boltzmann distribution of populations of spin levels in strong magnetic fields, on the EPR spectra of Mn_{Ga}^{2+}-O_{As}^{2-} in GaAs. The EPR spectra of Mn_{Ga}^{2+}-O_{As}^{2-} complexes and ionized Mn_{Ga}^{2+} acceptors were simulated for a temperature of 2.5 K and 10 K. A line width of 2 mT, which allows one to reveal the resolved hyperfine structure of manganese, was used in simulations.

itself (see Fig. 5, a), and the intensities of other transitions for orientation $\theta = 70°$ redistribute. With further increase in temperature, the observed spectrum should become symmetrical with respect to the central transition $-1/2 \rightarrow +1/2$. The signal of the Mn_{Ga}^{2+} EPR center varies little with increasing temperature: only the resolution of the hyperfine structure is enhanced. However, this demonstrates that the resolution of the HF structure at low temperatures is lower, since only the outermost transition $-5/2 \rightarrow -3/2$, where the spread of parameters of the crystal field manifests itself more profoundly than in the central transition $-1/2 \rightarrow +1/2$, is recorded. The latter transition is prevalent at higher temperatures.

4. Conclusion

The EPR spectra of two types of paramagnetic complexes were studied in the high-frequency range in strong magnetic fields at low temperatures. These complexes incorporate the same ionized acceptor A^- in the form of Mn_{Ga}^{2+} that interacts either with a delocalized hole with shallow levels (Mn_{Ga}^{2+}-SH complex) or with a hole localized at a diamagnetic oxygen impurity ion at the neighboring As site (Mn_{Ga}^{2+}-O_{As}^{2-} complex). Their models are shown in Fig. 2. The system of levels in a magnetic field was calculated for both complexes, the EPR transitions were identified, and the EPR spectra

observed in the context of a high Boltzmann factor, in which case only the lower energy levels are populated, were simulated. The conditions under which a complete diagram of energy levels may be derived from EPR data were determined. The correctness of the already proposed models with antiferromagnetic exchange interaction in the system of ionized manganese acceptor–shallow hole with lower level $F = 1$ was confirmed. The order of levels in the complex of ionized manganese acceptor–hole localized at oxygen with $S = 5/2$ was established. It was demonstrated that magnetic ordering is not established in the studied samples even in high magnetic fields and at temperatures down to 1.7 K.

Conflict of interest

The authors declare that they have no conflict of interest.

References

[1] A.V. Komarov, S.M. Ryabchenko, O.V. Terletskii, I.I. Zheru, R.D. Ivanchuk. Zh. Eksp. Teor. Fiz. **73**, 608 (1977). [Sov. Phys. JETP **46**, 318 (1977)].

[2] J.A. Gaj, R.R. Galazka, M. Nawrocki. Solid State Commun. **25**, 193 (1978).

[3] Semiconductor and Semimetals / Ed. J.K. Furdyna, J. Kossut. Academic, N.Y. (1988). V. 25.

[4] H. Ohno, A. Shen, F. Matsukura, A. Oiwa, A. Endo, S. Katsumoto, Y. Iye. Appl. Phys. Lett. **69**, 363 (1996).

[5] T. Dietl, H. Ohno. Rev. Mod. Phys. **86**, 187 (2014).

[6] J. Schneider, U. Kaufmann, W. Wilkening, M. Baeumler, F. Kohl. Phys. Rev. Lett. **59**, 240 (1987).

[7] V.F. Masterov, K.F. Shtel'makh, M.N. Barbashov, Sov. Phys. Semicond. **22**, _4_, 408 (1988).

[8] N.S. Averkiev, A.A. Gutkin, O.G. Krasikova, E.B. Osipov, M.A. Reshchikov, Sov. Phys. Semicond. **23**, 44 (1989).

[9] N.S. Averkiev, A.A. Gutkin, Phys. Solid State **60**, 2275 (2018).

[10] M. Glunk, J. Daeubler, L. Dreher, S. Schwaiger, W. Schoch, R. Sauer, W. Limmer, A. Brandlmaier, S.T.B. Goennenwein, C. Bihler, M.S. Brandt. Phys. Rev. B **79**, 195206 (2009).

[11] D. Bimberg. Phys. Rev. B **18**, 1794 (1978).

[12] V.F. Sapega, T. Ruf, M. Cardona. Phys. Status Solidi B **226**, 339 (2001).

[13] H.C. Averkiev, A.A. Gutkin, E.B. Osipov, M.A. Reshchikov. Sov. Phys. Solid State **30**, 438 (1988).

[14] M. Linnarsson, E. Janzén, B. Monemar, M. Kleverman, A. Thilderkvist. Phys. Rev. B **55**, 6938 (1997).

[15] N.P. Baran, V.M. Maksimenko, Yu.G. Semenov, V.Ya. Bratus', A.V. Markov. JETP Lett. **55**, 101 (1992).

[16] N. Almeleh, B. Goldstein. Phys. Rev. **12S**, 1568 (1962).

[17] R. Bleekrode, J. Dieleman, H.J. Vegter. Phys. Lett. **2**, 355 (1962).

[18] Y.J. Park, E.K. Kim, S.-K. Min, I.-W. Park, T.H. Yeom, H. Munekata, H. Kukimoto. J. Korean Phys. Society (Proc. Suppl.) **30**, S113 (1997).

[19] M. Pawłowsky, M. Piersa, A. Wołoś, M. Palczewska, G. Strzelecka, A. Hruban, J. Gosk, M. Kamińska, A. Twardowski. Acta Phys. Polonica A **108**, 825 (2005).